Removal Analysis and Ultrasonic Assisted Wire Electrical Discharge Grinding (UA-WEDG) Processes with Augmented Rotational Axis

Albert Wen-Jeng Hsue[1], Jun-Jie Wang[2], Yin Chuan[3]*

[1,2]Department of Mold and Die Engineering, National Kaohsiung University of Applied Sciences, Kaohsiung City, 807, Taiwan, R.O.C.

[3]Mold & Precision Machining Technology Section, Metal Industries Research and Development Centre, Kaohsiung City, 811, Taiwan, R.O.C.

**E-mail: albert.hsue@kuas.edu.tw*

Abstract - A rotational axis augmented to Wire Electrical Discharge Grinding (WEDG) processes and the dressing process assisted with ultrasonic vibration is reported. On its removal mechanism, a quantitative analysis based upon Wire-EDM discharge-angle was proposed to clarify fundamental understanding of the novel WEDG mechanism. The proposed analysis provides a better understanding for multi-axial WEDG for improving both the stability and the dressing efficiency. Because conventional WEDG usually resulted in rough surface and the significant consuming time was needed to achieve an acceptable quality. Therefore, an ultrasonic assisted UA-WEDG system associated with a small conic cup were then developed in this study to comedy these points. Its significant effects on improving machining efficiency and surface integrity of micro tools were verified experimentally.

Keywords - Wire-EDM discharge-angle, wire electrical discharge grinding (WEDG), ultrasonic assisted machining (UAM), micro-EDM.

I. INTRODUCTION

In the emerging micro-EDM manufacturing field, the most popular and reliable method for micro electrode forming is conducted through Wire Electrical Discharge Grinding (WEDG) process, which was developed by Prof. Masuzawa [1] in 1985. However, the original WEDG adopted only the two dimensional dressing capability for micro-electrode. Therefore, more axes of the WEDG would be helpful and eagerly needed, for example, to meet the requirements of the cylindrical works or specific curved-surface introduced in [2, 3]. Therefore, by similar design concept to cylindrical-WIRE-EDM in commercial macro scale [4, 5], the rotational mechanism was further reinvented to apply to the WEDG system for dressing micro electrodes. Furthermore, their fundamental study will also be needed for better design of micro-EDM processes.

Moreover, conventional WEDG usually resulted in rough surface similar to bamboo's knots after high feed-rate dressing. Besides the rotational axis was augmented to the original WEDG, an ultrasonic assisted UA-WEDG system was then developed in this study to improve the machining efficiency and surface integrity.

The rotational axis was designed to provide the rotation capability for wire electrode along the X-axis (A-axis) for convenient dressing and observation. In this paper, the novel rotation spindle was conducted through an AC-servo motor associated with a planet reduction gear system. A much simpler and intuitive scheme than past research on cylindrical wire-EDM was proposed for its removal analysis. These fundamental removal analysis and application were developed based upon wire-EDM's discharge-angle [6, 7]. The discharge-angle was defined as the angular range spanned by very short period of EDM working time, where the wire-EDMed removal was taken as the volume swept by such an angle.

Ultrasonic assisted WEDG was quite rare in the past, except ultrasonic assisted electrical discharge grinding (US-ED-G) and micro-hole drilling [8, 9]. It was conducted through attaching an ultrasonic head to an EDG wheel, causing high frequency vibration along the wheel's axial direction. It was reported even for very hard work material TiB_2, small peak current of EDG can be helpful to reduce its grinding resistance. And much better effects were reported with larger peak current. Recent study also presented an experimental investigation on cylindrical wire electrical discharge turning process [10].

In this study, two types of vibration were conducted to project vibration waves into the dielectric fluid and to the wire electrode, respectively. Then, comparison studies were also conducted and discussed. These experimental results provided comparisons for original WEDG dressing effects without vibration-assisted methods.

II. DESIGN AND SETUP OF THE UA-WEDG

An original micro-EDM machine (model MD-22) was set up by a local EDM machine builder, Aristech, and a research center, MIRDC, in Taiwan. Each axis of such a micro-EDM machine was driven by linear motor direct-drive, and guided by aero-static bearings with granite support.

In the lab, a retrofitted WEDG system, as shown in the left of Fig. 1, was attached to the machine table of micro-EDM machine. The WEDG system's wire was conducted through a half-disk made of tool steel with v-slit. By choosing proper guides and wire tension, the thin wire of 100 micron and even 50 micron diameters can be adopted as the tool electrodes.

As shown in the following Fig. 1, the rotational axis was designed along the x-axis of WEDG mechanism for dressing simplicity. A 100W of AC-servo motor with reduction gear system served as the rotational power and its control was conducted through a PC-based motion card.

Since its configuration is similar to cylindrical wire-EDM, the fundamental analysis can be induced from cylindrical WIRE-EDM to this case. It is obvious that the removal mechanism and the machining stability are even more critical in this micro scale processes than macro wire-EDM. Because small un-cut volume might cause short-circuit and result in unstable. However, since its wire electrode suffered much less discharge energy, its removal rate might be obtained in a much precision way than macro wire-EDM process because the wire deflection may be considered as negligible in this case. Therefore, the fundamental analysis may be closer to the real practice, and it may contribute to a good suggestion for improving not only the dressing stability but also the precision and the surface quality.

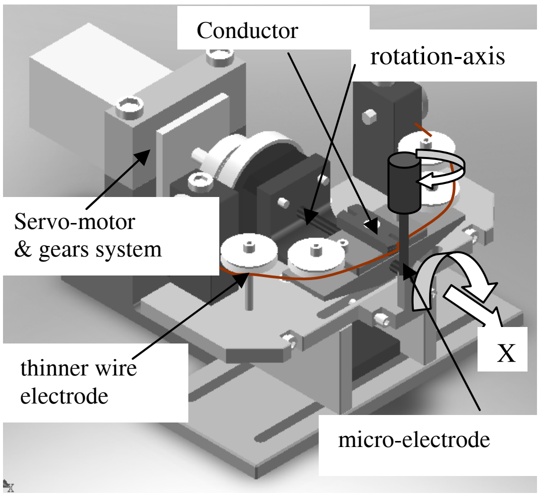

Fig. 1. Solid model of the novel design for augmented rotational axis to a general WEDG system.

A vibrator with ultrasonic head was realized for micro electrode dressing processes as shown in Fig. 2. Such an ultrasonic vibrator aligned along an inclined angle of 45^o from horizontal and was developed for two vibration modes. Namely, they are operated to disturb the dielectric fluid and to vibrate the wire electrode itself directly, respectively.

The design concept revealed the rotational axis can provided from -15^o to 15^o of inclination for WEDG wire. And the ultrasonic head was also been inclined along with the level table. In the first type of ultrasonic assisted vibration, the ultrasonic assisted head was submerged into the dielectric fluid contained in a conic cup. To provide a better debris extruding processes during WEDG, this cup was machined into a small conic container of about 40 mm diameters for better shock-wave effects. In the second vibration assistance type, the tip of ultrasonic head was milled into a short slit and attached to the threading wire.

In order to associate WEDG with the effect of ultrasonic vibration for improving efficiency and quality, ultrasonic frequency with about 42.8KHZ was tuned as shown in the following figure 3. The ultrasonic transducer is driven by a piezo-electric actuator, and then amplified into the end effecter with a stainless steel horn shaft.

Such a small working zone was observed with a 12x microscope video system, as shown in Fig. 4. Detailed feed direction of WEDG wire is aligned along X-axis and the augmented axis allows rotation in A-axis direction. The micro-electrode is fed downward along the Z-axis with its own spindle. Both X, Y and Z–axes are driven by linear motors, supported by aero-static bearing.

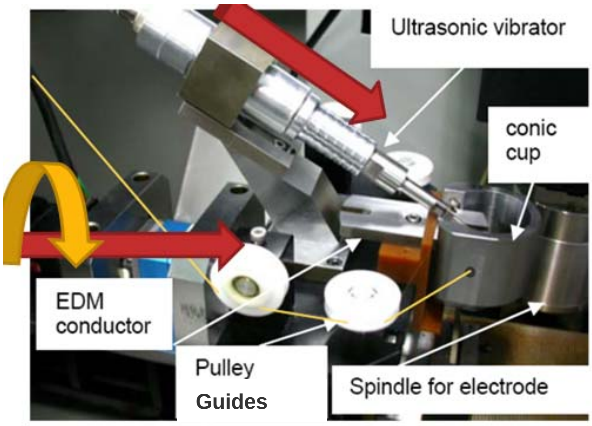

Fig. 2. Ultrasonic vibration assisted mechanism setup for the multi-axial WEDG system (UA-WEDG).

Fig. 3. Setup of the ultrasonic vibrator and its power supply.

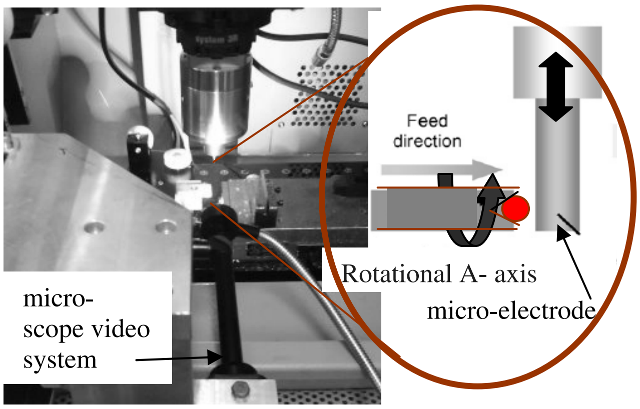

Fig. 4. Assembled multi-axial WEDG on the micro-EDM machine with microscope video system.

III. MATERIAL REMOVAL ANALYSIS

As shown in Fig. 5, the WIRE-EDM discharge angle is defined as the angular range spanned by EDM discharge sparks along the front surface of wire electrode. Based upon the WIRE-EDM removal model presented in [7, 8], two points were summarized as, point (1): the sweeping width, W is equal to cosine projection of the arc along the discharge angle. And point (2): the swept area during a sampling period Δt is formulated as $Wu\Delta t$.

Removal analysis for cylindrical WIRE-EDM is started from the first integral theorem of Pappus, which dedicated to the integral of sweeping volume from revolution of a fixed cross-section area. Therefore, the removal volume formatted by revolving section with the centric distance with respect to (w.r.t.) the rotational axis was taken to represent the removal swept area. A general bulking case for an arbitrary incline angle is proposed. Slitting perpendicular to the axis and bulking along the axis were considered as special cases with ninety or zero degrees of incline angles, respectively.

A. General Bulking with an Inclined Angle

Similar to the traditional lathe, the cylindrical wire-EDM and rotational WEDG process have the capability of free forming on a work piece shaft. Consider the case of generally cylindrical forming process, where the feed direction is inclined an angle, α w. r. t. the revolution axis at a moment as shown in the Fig. 6. Its discharge-angle is directly related to the incline angle by

$$C_\theta = \alpha + \frac{\pi}{2} \tag{1}$$

As the wire moves forward by a distance of $\Delta\lambda$, its removal includes hatched bulks volume reaches from the bottom of wire surface to the outer radius of work piece. Its typical feature can be described by discharge-angle of WIRE-EDM along a circular arc as shown in area ABCFED. The small removal volume in such a differential distance can be obtained by summing swept volumes of V_{ABCD} and V_{CDEF}. Where,

$$V_{ABCD} = \pi(R^2 - r^2)\Delta x + 2\pi(r - \frac{\Delta r}{3})\frac{\Delta r \Delta x}{2} \tag{2}$$

The relationship between Δx, Δr, and $\Delta\lambda$ are shown in the right of Fig. 6. For volume V_{CDEF}, suppose a moving coordinate $(\bar{x}, \bar{y})$ located at wire center O, the removal can also be derived by coordinated rotation into left of the Fig. A in the Appendix. Then, the new y-direction's centroid of the hatched area A_2 w. r. t. the moving coordinate is,

$$\bar{y}_2 = \{-\frac{1}{2}\Delta\lambda^2(S + \frac{r_e}{2\Delta\lambda}\sin 2\alpha) - \frac{1}{4}\pi r_e[\Delta\lambda(1 + \frac{2\alpha}{\pi}) + \frac{4}{3\pi}r_e S] + \frac{1}{3}r_e^2 S\}/(S\,\Delta\lambda) \tag{3}$$

Where, factor S is defined as the cosine projection of discharge angle as stated in Eq. (A.5) of the Appendix. Moreover, let the coordinate system O$(\bar{x}, \bar{y})$ rotate back to the α angular position, then, the actual centroid of hatched area can be obtained as follows:

$$\begin{aligned}\bar{y}_2' &= \bar{x}_2\sin(\frac{\pi}{2} - \alpha) + \bar{y}_2\cos(\frac{\pi}{2} - \alpha) \\ &= -\frac{1}{2}r_e(1 - \sin\alpha)\cos\alpha + \{-\frac{1}{2}\Delta\lambda^2(S + \frac{r_e}{2\Delta\lambda}\sin 2\alpha) - \\ &\quad \frac{1}{4}\pi r_e[\Delta\lambda(1 + \frac{2\alpha}{\pi}) + \frac{4}{3\pi}r_e S] + \frac{1}{3}r_e^2 S\}\sin\alpha \Big/ S\Delta\lambda\end{aligned} \tag{4}$$

$$\bar{x}_2 = -\frac{1}{2}r_e(1 + \cos C_\theta) \tag{5}$$

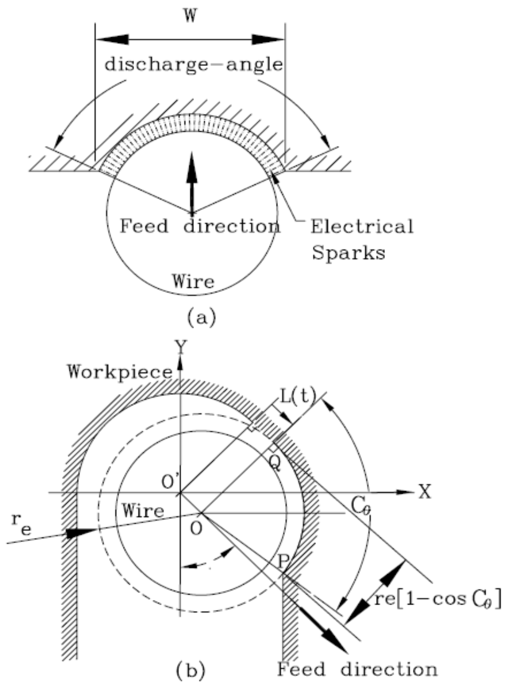

Fig. 5. (a) Definition of discharge-angle C_θ in wire-EDM top view. (b) ideal removal model for corner cutting.

Hence, by Pappus theorem, the removal in front of the wire is derived as,

$$V_{CDEF} = 2\pi A_2(r + \bar{y}_2') \tag{6}$$

Therefore, the general removing process in such a bulking removal process is then obtained by,

$$\begin{aligned}\Delta V &= V_{ABCD} + V_{CDEF} \\ &= \pi\Delta x(R^2 - r^2) + 2\pi(r - \frac{\Delta r}{3})\frac{\Delta r\Delta x}{2} + 2\pi S r_e\Delta\lambda(r + \bar{y}_2')\end{aligned} \tag{7}$$

And, the theoretical removal rate is then derived as,

$$\begin{aligned}MRR &= \pi(R^2 - r^2)u\cos\alpha + \lim_{\Delta t \to 0}\{\pi(r - \frac{u\Delta t\cdot\sin\alpha}{3})\frac{u\Delta t\cdot\sin 2\alpha}{2} + \\ &\quad 2\pi S r_e(r + \bar{y}_2')\}u\end{aligned} \tag{8}$$

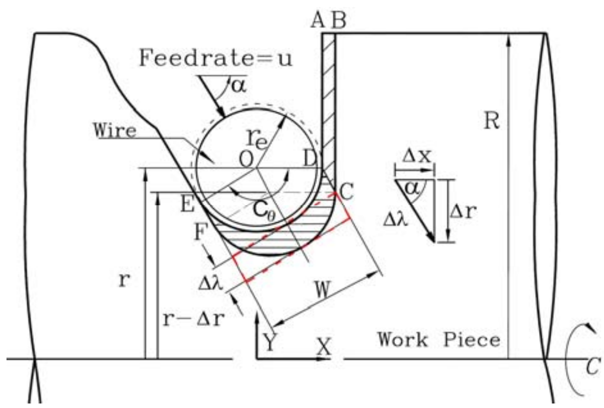

Fig. 6. General removal model for WEDG an inclined α angle of wire with respect to the revolution axis.

B. Removal Simulation and Verification

For verification of the analysis, several general bulk cuttings with various inclined angles were conducted with constant feed rate. The simulation were conducted through a commercial WIRE-EDM with wire diameter of 0.25 mm. Cylindrical rod with diameter of 10 mm and of 150 mm length was chosen as workpiece. From Eq. (8), the dominate factors for MRR are feedrate and wire-EDM discharge-angle. Let's set the inclined angle from 20, 30, 45, to 60 degrees for discussion. And feedrate of 6.0 mm/min with effective discharge radius of 0.145 mm are also assumed.

The theoretical removal rates in mm^3/min under several conditions were computed as shown in the Fig. 7. In this simulation, a dummy variable is defined at outer radius with respect to the revolving axis. The initial status of wire-EDM is represented as wire located at origin point of X, outside the rod surface.

It is evident that as the incline angle increases, the removal rate increases abruptly in smaller lateral displacement, x(t), and increases gently in larger x(t). But the maximum removal rate decreases as angles increases. It is also evident that the MRR saturates much sooner for larger incline angle as wire moves toward axis. Therefore, there is some intersection points occurred in steep angles, which indicates some sorts of cross-over phenomena occurred in saturation zone, regarding various machining efficiency.

Abruptly increasing MRR of each angle implies that increasing discharges power or discharge frequency for iso-energy machine is needed. Therefore, important suggestion arose from this figure that the federates and the discharge off-time should be adjusted according to the MRR profiles to meet the efficiency and some surface integrity requirements, as suggested in the work [6-7].

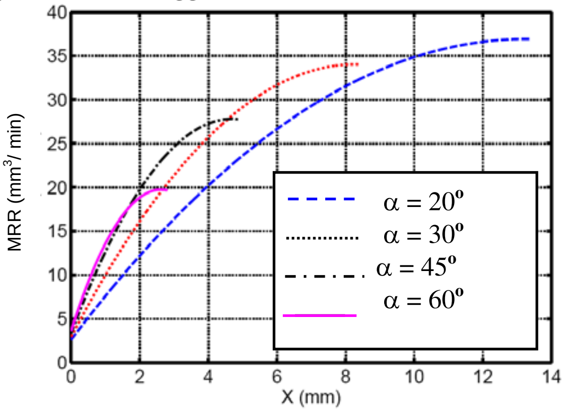

Fig. 7. Theoretical removal rates (MRR) for several inclined angles from 20° to 60°.

However, the strict assumption regards of simplicity of this analysis scheme may limit the application of the model. And the 0.25 mm diameter of wire electrodes is different from the micro wire used in WEDG situation. But similar configuration and assumption are still suitable. Although thinner wire is adopted in WEDG, the much shorter span of wire maintains the rigid assumption. Therefore, it still provides comprehensive understanding to the novel WEDG mechanism, and further derivation is still urgently needed in the near future.

IV. EXPERIMENTAL RESULTS

The material of target micro tool is conducted with 0.5mm in diameter of tungsten carbide (with grain size of 600nm). The assistance of ultrasonic vibration is planned into two types: vibration exerted on wire electrode, and vibration on dielectric fluid. Table I revealed the operation conditions for the WEDG and the rotational WEDG with ultrasonic assistance. In which, the feed rate of X-axis was controlled by gap voltage.

Table I. Operation conditions for the WEDG

V_O (V)	I_p (A)	T_{ON} (μS)	T_{Off} (μS)	X-asis Feedrate mode	Z-axis Feedrate (mm/min)	Flush
120	0.5	0.5	0.5	G95	0.2	N/A

A. Regular Rotational WEDG Results

As shown in the Fig. 8, the dressed micro rod with proposed WEDG in a horizontal attitude (without rotation) was measured. The raw material of 500 μm diameter was adopted for micro electrode. In Figure 8 (a) a micro rod of 50 μm diameter was obtained by two additional finishing processes. They look much smoother because out of focus and some dielectric oil remained on the surface. But the Figure 8 (b) shows a necking at shaft step. That might be resulted from the second finishing processes besides original WEDG process.

(a) (b)

Fig 8. (a) Micro-rod of 50 μm dia. is dressed by the proposed mechanism, and (b) its step neck near the raw material of 500 μm .

As shown in the figure 9, fine rods of 40 μm and 22 μm conducted by the proposed WEDG mechanism were further achieved. The dressing effect of fine rods from 100 ~40 μm looks fairly well, but a smaller rod such as 22 μm

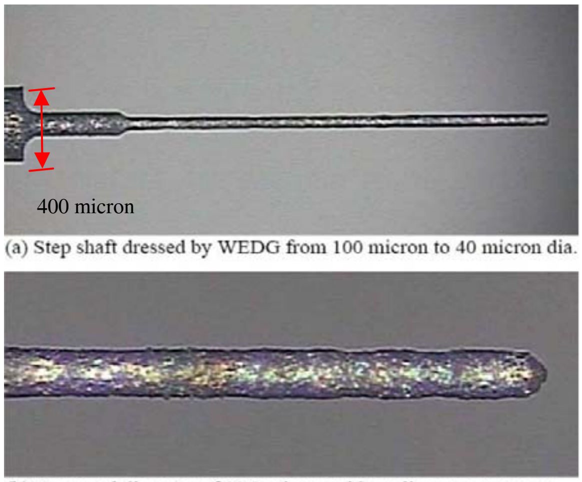

(a) Step shaft dressed by WEDG from 100 micron to 40 micron dia.

(b) Averaged diameter of 22.2 micron with on-line measurement

Fig. 9. The dressing effects on fine rods of 40 about μm and 22 μm by the proposed WEDG mechanism.

reveals some sort of surface straightness problem. The surface profile of very thin rod may be caused by higher federate of Z-axis and vibration of wire electrode, which made the relative movement of both electrodes vary and the non-uniform EDM removal.

B. Results of WEDG without/with Ultrasonic UAM

As shown in the figure 10, the dressed micro rod with general standard WEDG, and the proposed WEDG in a horizontal attitude was measured and compared. But general WEDG is conducted with free flushing; and the UA-WEDG is with target tool submerged into the proposed conic cup. Both are dressed with 5 cuts from 0.5 mm to 0.08 mm. The general WEDG took about 95 minutes, and the proposed WEDG took only 65.5 minutes with the same servo control (G95 mode). It saved up to about 32% of consuming time. Moreover, the figure 10(b) shows much sharper/clear shape at the last shaft step than figure 10(a). That might be resulted from better flushing process at the last cut. Because the vibration wave of ultrasonic vibrator can be constrained and reflected in the small conic cup.

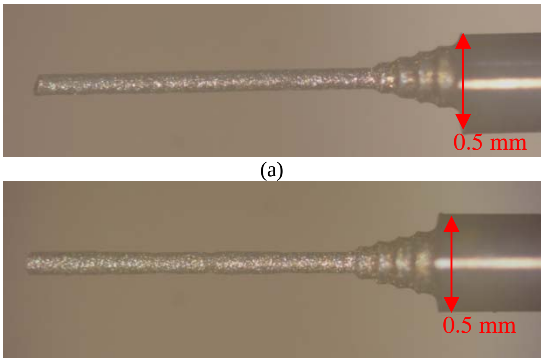

(b)

Fig. 10 Comparison of the dressing results, (a) with general standard WEDG (95 min 14 S), (b) with UA-WEDG (65 min 27 S), dressed into 100 micron dia wih 1.6 mm long.

The SEM photo of the sample in previous test was also observed in the following SEM photo in figure 11. The shape integrity looks fairly well. But dressed shape's surface looks quite obviously rough; because of rather high peak current was conducted by 500 mA in this experiment.

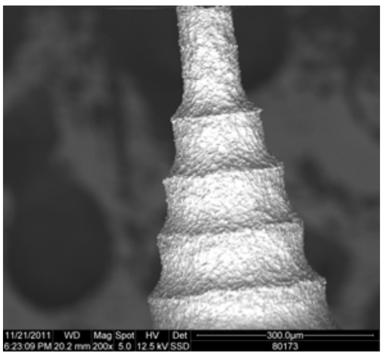

Fig. 11. SEM photo of the rod with UA-WEDG dressing into 0.1 mm diameter from 0.5 mm.

The smaller peak current of 50 mA is on the go in the lab. Therefore, much smaller diameter can easily been conducted with this mechanism, for example, 30 micron in end shaft. But for the application of EDM micro-milling, it is still not practical to conducted too thin tool electrode up to date in the lab. Therefore, we proposed a micro tool of about 70 micron in diameter to micro machining tests in the next experiments on EDM milling.

As revealed in the figure 12, lateral view and end view for a long pitch of screw dressed by the proposed multi-axial UA-WEDG system were measured. Although it was offset form the Z-spindle center line, the screw was machined into quite an integrated shape. This result verifies the effectiveness of the proposed multi-axial dressing capability by the novel WEDG mechanism.

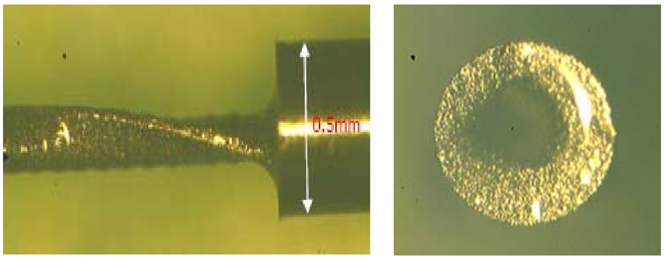

(a) (b)

Fig. 12. Lateral view and end view for a long pitch of screw conducted by the proposed multi-axial UA-WEDG system.

V. CONCLUSION

Development and removal analysis of the novel multi-axial WEDG processes assisted by ultrasonic vibration are reported in this study. A geometrical model on material removal rate and preliminary implementations for the multi-axial WEDG tests were presented in this report. Some points were summarized as;

1. This report has provided fundamental understanding for cylindrical WEDG process in generalized micro tools forming.
2. Abruptly increasing MRR in the general removal model implies a gap control strategy is eagerly required for machining stability and efficiency.

By introducing an ultrasonic vibrator to multi-axial WEDG system, the machining performance was improved significantly. Specifically, by adding vibration to the wire electrode directly, the dressing surface integrity of micro rod was improved over vibrating the dielectric fluid or without ultrasonic assistance. Because the debris expelling processes of EDM was improved by ultrasonic assistance, and the vibration waves are constrained in a small conic cup, the machining time needed to dress the same micro tool is significantly saved.

ACKNOLWEDGEMENT

Support from National Science Council under Grant NSC 100-2221-E-151-070 and technology supports from Dr. F-C Hsu of MIRDC Taiwan, and suggestion from Dr. T-H of Dahan Institute of Technology are well acknowledged.

REFERENCE

[1] T. Masuzawa, M. Fujino, and K. Kobayashi, *Wire Electro Discharge Grinding for Micro Machining*, Ann. CIRP Vol.34 (1985), 431–434.

[2] Internet Web Information on http://www.fanuc.co.jp/en/product/robocut/alphaic5/index.html, & http://www.fanuc.co.jp/en/product/robocut/alphaic5/toolcutting/toolcutting.html#screen, (2010)

[3] Y. S. Liao, S. T. Chen, and C. S. Lin, *Development of a high precision tabletop versatile CNC wire-EDM for making intricate micro parts*, J. Micromech. Microeng. 15 (2005), 245–253.

[4] J. Qu, A-J. Shin, and R-O. *Scattergood, Development of the Cylindrical Wire Electrical Discharge Machining Process, Part1: Concept, Design, and Material Removal Rate*, J. Manuf. Sci. and Eng., Trans. ASME Vol.124 (2002),702-707.

[5] J. Qu, A-J. Shin, and R-O. Scattergood, *Development of the Cylindrical Wire Electrical Discharge Machining Process, Part2: Surface Integrity & Roundness*, J. Manuf. Sci. and Eng., Trans. ASME Vol.124 (2002),708-714.

[6] W. J. (Albert) Hsue, Y. S. Liao, and S. S. Lu, *Fundamental Geometry Analysis of Wire Electrical Discharge Machining in Corner Cutting*, Int. J. Mach. Tools & Manuf. Vol.39(4) (1998), 651-667.

[7] W. J. (Albert) Hsue, Y. S. Liao and S. S. Lu, *A Study of Corner Control Strategy of Wire-EDM Based on Quantitative MRR Analysis*, Int. J. Elec. Machining, No.4 (1999), 33-39.

[8] H. Onikura, *Effect of Ultrasonic Vibration on Machininh Accuracy in Micro Drilling*, Int. I. Japan Soc. Eng, Vol.30-3, (1996) 210-216.

[9] J. C. Hung, J.-K. Lin, B.-H. Yan, H.-S. Liu and P.-H. Ho, *Using a helical micro-tool in micro-EDM combined with ultrasonic vibration for micro-hole machining*, J. Micromech. Microeng. 16 (2006) 2705–2713.

[10] M. J. Haddad, F. Alihoseini, M. Hadi, M. Hadad, A. F. Tehrani, and A. Mohammadi, *An experimental investigation of cylindrical wire electrical discharge turning process*, Int. J. Adv Manuf Technol 46, (2010) 1119–1132.

APPENDIX

As shown in left of Fig. A, suppose the moving coordinate system $O(\bar{X}, \bar{Y})$ with wire's removal was rotated clockwise from the Fig. 6, so that the feed direction is perpendicular to the revolution axis. The discussed total area, *A*, of polygon OEFCD is the summation of the arc sector A_1 of ODE and the area A_2 swept by the discharge-angle denoted by the hatched area. The area can easily be obtained by the concept of discharge-angle with the centric to be determined as followed.

$$A_1 = \frac{1}{2} r_e^2 C_\theta, \quad A_2 = r_e[1-\cos C_\theta]\Delta\lambda \qquad \text{(A.1)}$$

with centric,

$$\bar{y}_1 = -\frac{2}{3C_\theta} r_e(1-\cos C_\theta) \qquad \text{(A.2)}$$

and $\bar{y}_2$ is unknown. And then,

$$A\bar{y} = A_1\bar{y}_1 + A_2\bar{y}_2 \qquad \text{(A.3)}$$

On the other hand, as shown in the right of Fig. A, the total area *A* can also be taken as the summation of a square A_I, a parallelogram A_{II}, a quarter circular sector A_{III} and an arc sector denoted as A_{IV}. Since all of the small areas are basic geometries, the aerial momentum in the above equations can also be taken as following summation.

$$A\bar{y} = -\frac{1}{2} r_e \Delta\lambda^2 \left(1+\sin\alpha + \frac{r_e}{2\Delta\lambda}\sin 2\alpha\right) - \frac{1}{4}\pi r_e^2\left[\Delta\lambda\left(1+\frac{2\alpha}{\pi}\right) + \frac{4}{3\pi} r_e(1+\sin\alpha)\right] \qquad \text{(A.4)}$$

For simplicity, let S denote the cosine projection factor of arc length swept by discharge-angle,

$$S = 1-\cos C_\theta = 1+\sin\alpha \qquad \text{(A.5)}$$

Then the centroid of the hatched area w. r. t. the moving coordinate can be determined from (A.3) and (A.4) as

$$\overline{y_2} = \left\{-\frac{1}{2}\Delta\lambda^2\left(S+\frac{r_e}{2\Delta\lambda}\sin 2\alpha\right) - \frac{1}{4}\pi r_e\left[\Delta\lambda\left(1+\frac{2\alpha}{\pi}\right) + \frac{4}{3\pi} r_e S\right] + \frac{1}{3} r_e^2 S\right\}/(S\Delta\lambda) \qquad \text{(A.6)}$$

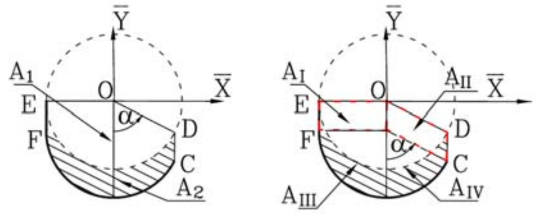

Fig. A. Computation model for sweeping area with coordinate transformation for multi-axial WEDG mechanism.